

Monitoring the Corrosion Rate of Carbon Steel under a Single Droplet of NaCl

G A. EL-Mahdy^{1,2,*}, Hamad A. Al-Lohedan, Zuhir Issa

¹ Surfactant Research Chair, Chemistry Department, College of Science, King Saud University, P.O.Box - 2455, Riyadh - 11451, Saudi Arabia

² Chemistry department, Faculty of Science, Helwan University, Helwan 11795,

Egypt

*E-mail: gamalmah2000@yahoo.com

Received: 26 August 2014 / Accepted: 5 October 2014 / Published: 28 October 2014

A new design for an experimental set-up is proposed for monitoring the contact angle, droplet height, base diameter, corrosion rate and volume loss under a single droplet of NaCl placed gently on carbon steel surface. The monitoring results indicated that the contact angle and droplet height decreased while the volume losses and the corrosion rate increased as holding time progressed. The droplet diameter remains practically constant over a holding lifetime of the drop. A mechanism describing the successive stages of a corrosion process under a single droplet of NaCl is proposed.

Keywords: Carbon steel, polarization resistance, contact angle, droplet height, EIS

1. INTRODUCTION

The micro-droplets formation on metal surfaces is closely related to atmospheric corrosion [1]. It was found that micro-droplets could only form in a corrosive combination of metal and electrolyte droplet. The formation of droplet is easier at higher relative humidity (RH) than that formed at lower one [2, 3]. The droplets might be different in terms of oxygen depletion, ion migration, consumption of reactants, precipitation of corrosion products and establishment of anodic and cathodic zones. The corrosion of metal under fine size droplet is an important to an atmospheric corrosion process due to the pathway of oxygen diffusion, which is relatively short for fine size droplets and the ratio of droplet volume to exposed metal surface area, which is proportional to the droplet radius. It was reported previously that as the droplet radius decreases the relative total number of active species to reactive area will decrease [4]. The corrosion process under fine size droplets of various pH values, acidifying agents and concentration variations have been investigated to demonstrate the role of ions

from different dissociated salt [5-6]. Atmospheric corrosion in different urban and industrial atmospheres variation imitates the atmospheres found in distinct marine and industrial environments [7-9]. The aim of the present work is to investigate the role of a single droplet (NaCl) characterizations on the corrosion rate of carbon steel using electrochemical impedance spectroscopy (EIS) and drop shape analyzer (DSA) and its mechanism will be discussed.

2. EXPERIMENTAL PROCEDURE

2.1. Material and electrode preparation

Two-electrode cell configuration was fabricated from carbon steel sheet with dimensions of 0.1 mm (width) and 10 mm (length) and was placed 0.1 mm apart, in an epoxy resin. The cell was placed horizontally facing upward, in an acrylic vessel. The electrode was abraded mechanically with SiC paper with differing grades of up to # 2000 mesh, and then cleaned with ethanol in an ultrasonic bath.

2.2 Electrochemical impedance spectroscopy (EIS)

The impedance measurement was conducted at 10 kHz and 10mHz, using multichannel Solartron system 1470E. The polarization resistance (R_p) was determined by subtracting the high frequency impedance at 10 kHz from the low frequency impedance at 10 mHz.

2.3. Monitoring the droplet characteristics

The variations in droplet height, contact angle, base diameter and volume loss and during the progress of corrosion process will be monitored using a drop shape analysis system (DSA-100, Kruss, Germany) with analysis software DSA4 software (V.1.0-03).

2.3. Corrosion products Morphology

The morphology of the corrosion products was examined by utilizing optical microscopy (Olympus BX-53) fitted with DP72 digital camera). Images were processed using Olympus CellSens v1.6.

3. RESULTS AND DISCUSSION

3.1 Contact angle (wettability) measurement

Fig. 1 shows droplet contact angles as a function of time. The contact angle continually decreases throughout the portion of the evaporation from ~ 100 to $\sim 94^\circ$. It decreases faster as the

droplet approaches a thin film where three-dimensional motion of the droplet begins to occur. In addition, the decrease in contact angle may be attributed to the precipitation of the corrosion products, which have effective anticorrosion properties.

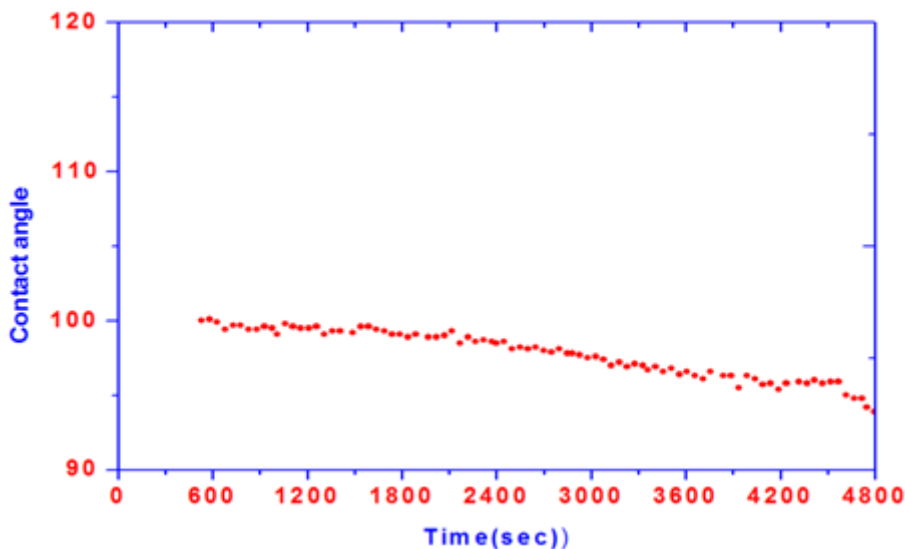


Figure 1. Variation of contact angle with time

Therefore, it is reasonable to conclude that the precipitation of the corrosion products during the last stage of monitoring with low wettability was able to effectively prevent the chloride ion from absorbing onto the substrate surface. Hence, it exhibits protective layer against corrosion. The carbon steel surface–liquid contact area as well as the chemical and physical nature of a surface have a direct influence on the rates of steel corrosion [10]. In addition, the liquid–vapour interface area controls the extent of oxygen/gas diffusion and controls the evaporation process.

3.2 Monitoring the volume losses and the droplet height

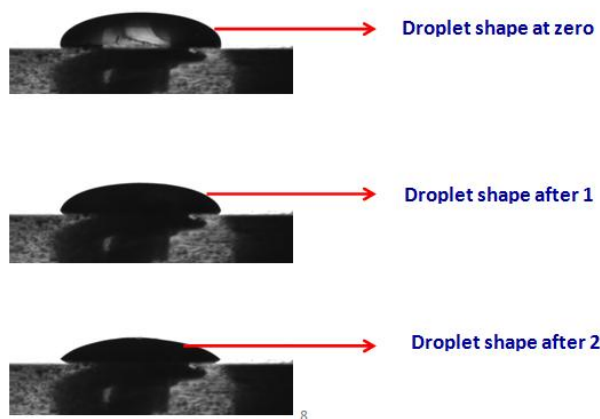


Figure 2. Sequences of droplet shape at different holding times

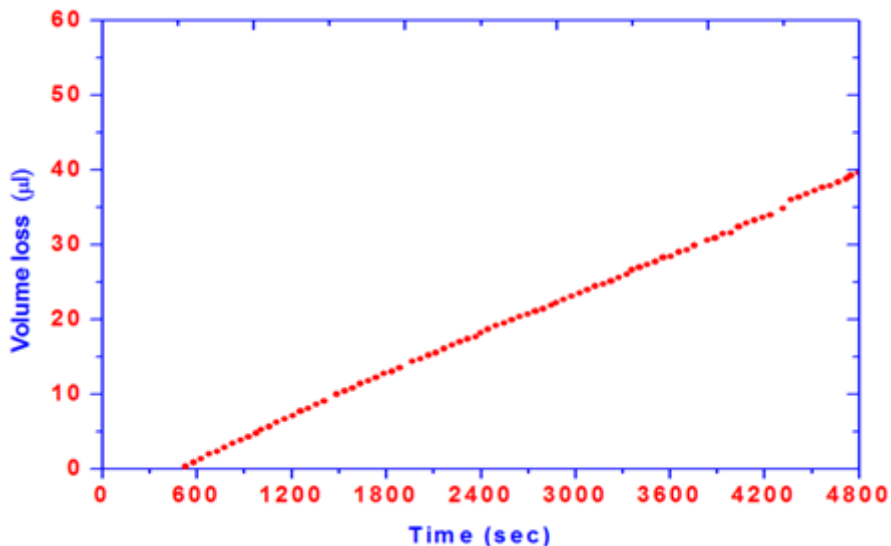


Figure 3. Variation of volume loss with time.

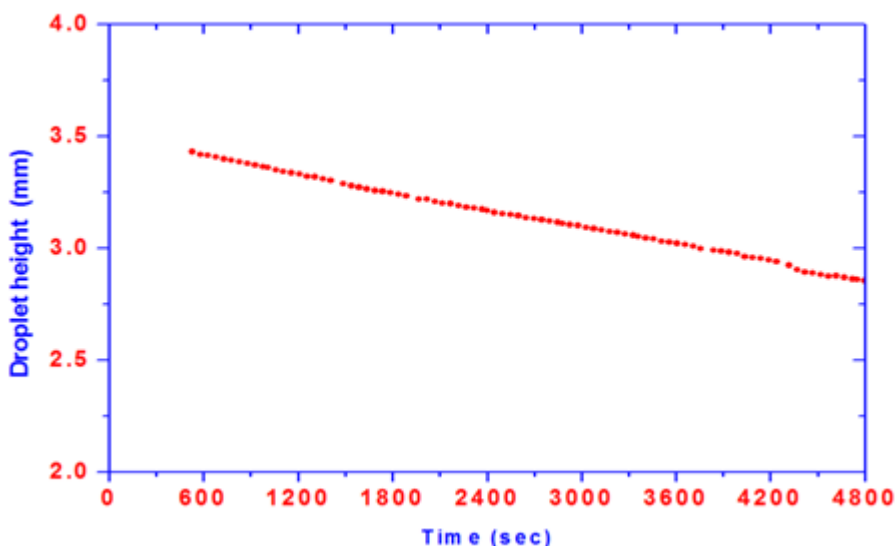


Figure 4. Monitoring data of droplet height with time

Fig. 2 shows a sequence of a sessile drop shape at different holding times during evaporation of a single drop of NaCl placed gently on CS surface. The monitoring data for volume losses and droplet heights as a function of time are shown in figures 3 and 4, respectively. The droplet height continually dropped, while the volume losses increased as droplet holding time progressed. The height of the NaCl droplet decreases nearly uniformly during the evaporation process. The results can be explained on the basis of water evaporation from the droplet, which increases as holding time progressed leading to increase the volume loss and decrease the droplet height. One can estimate the volume losses for drops with a known diameter by extrapolation of the data shown in Fig. 4 to zero height. It seems that the evaporation proceeds from the central part to the periphery along the cross-fin

direction. Fig. 5 shows the constancy of the droplet diameter with holding time. The droplet diameter remains practically constant over a holding lifetime of the drop. The droplet diameter shows an appreciable decrease at the end of the drop's lifetime. Fig. 2 confirms the constancy of the drop's width during evaporation.

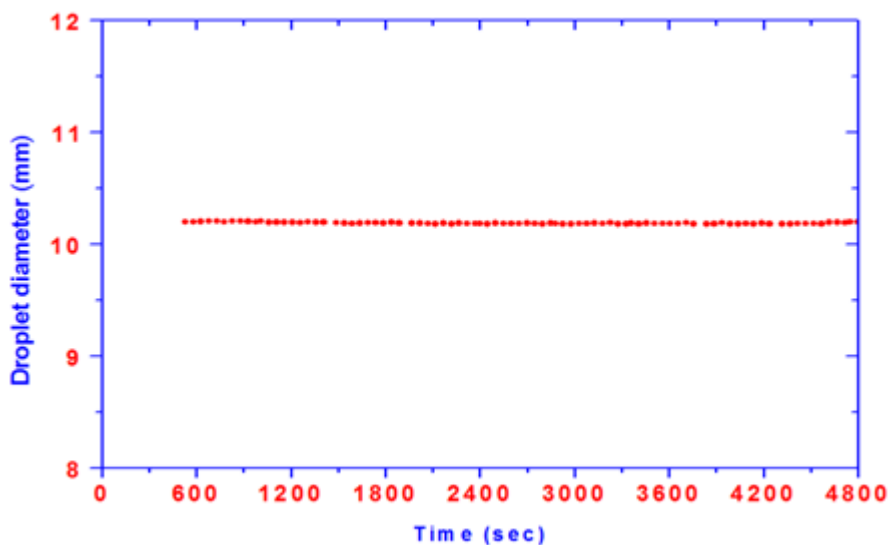


Figure 5. Constancy of the droplet diameter with holding time

3.3. Mechanism of corrosion process inside the droplet

Corrosion of carbon steel under a single droplet of NaCl is modeled with an equivalent circuit called a Randles circuit, which is made of a double-layer capacitance (C_{dl}) in parallel with a polarization resistance (R_p) resistor and connected in series with a electrolyte solution resistor (R_s). The impedance (Z) depends on the polarization resistance (R_p), the solution resistance (R_s), the capacitance of the electrical double layer. Electrochemical impedance spectroscopy (EIS) is applied to determine the influence of the droplet height on the corrosion behavior of carbon steel. The polarization resistance R_p and thus the corrosion rate can be obtained using electrochemical impedance measurements (EIS) by measuring at two different frequencies: Z_H (high frequency of about 10 kHz) and Z_L (low frequency of about 10 mHz) [11-22]. The polarisation resistance R_p is obtained by subtracting Z_H from Z_L , based on the assumption that high frequency impedance gives the solution resistance and low frequency impedance provides a sum of solution resistance and polarization resistance. Fig. 6 shows the monitoring data of $1/R_p$ versus the holding time. It is known that the polarization resistance (R_p) is inversely proportional to the corrosion rate (I_{corr}) according to Stern-Geary equation [23]:

$$\text{Corrosion rate} = K / R_p \tag{1}$$

$$K = \frac{b_a b_c}{2.303(b_a + b_c)} \tag{2}$$

where b_a and b_c represent anodic and cathodic Tafel slope, respectively.

The corrosion during the initial stage of droplet holding time is controlled by anodic dissolution of iron while the droplet height is high. As holding time progressed the corrosion rate is controlled by oxygen reduction, which enhanced by oxygen diffusion through a short path of the droplet with low droplet height.

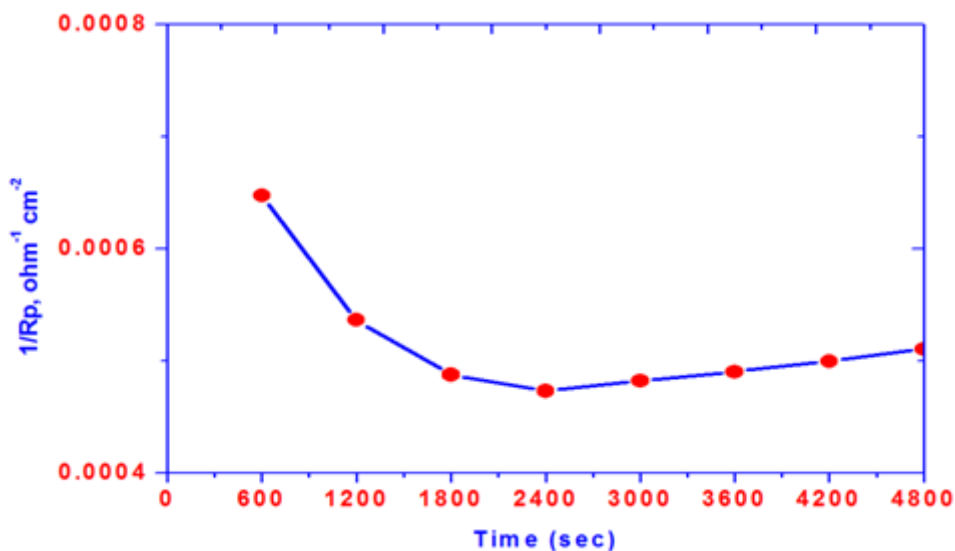


Figure 6. Monitoring data of reciprocal of polarization resistance with time.

It can be concluded that as the droplet height decreases the cathodic reduction of oxygen increases and generated negative charges leading to the decrease of liquid-metal interfacial energy and the acceleration of the water evaporation from primary-droplet, which might be one of the causes for an increase in the corrosion rate and a decrease of contact angle as holding time progressed. Generally the mechanism of carbon steel corrosion under droplets have a sequence of reactions including: the dissolution of the oxide film followed by dissolution of underlying surface and eventually precipitation of the corrosion products under a stable drop and in an evaporating drop. The corrosion process can be subdivided into two stages. The initial stage is dissolution of native oxide film followed by dissolution of underlying substrate surface. The second stage includes the corrosion process under small droplet height, which may develop corrosion products in different parts of the droplet as a response to different local conditions [24]. Chloride ion concentration effects play an important role in the dissolution of the steel and is related to the anodic area and thus to droplet contact surface area. The production of Fe^{2+} is likely controlled by the dissolution of steel (net anode at the droplet center).

The net cathode reaction is a reduction of oxygen, which enhanced as the droplet height decreases and providing a short path for oxygen diffusion, As a result of continuous water evaporation and decreasing the droplet height as holding time progressed the Fe^{2+} concentration in fine droplets may reach a sufficient level to cause a quick precipitation of the corrosion products.

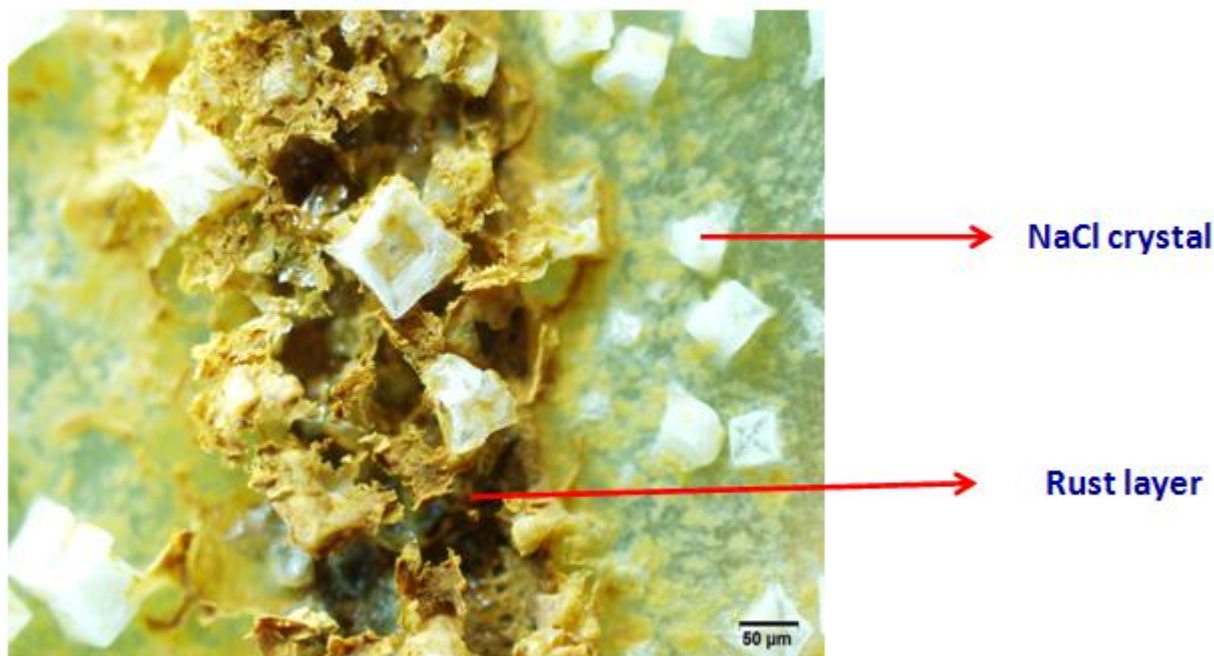


Figure 7. Photomicrograph of the formed corrosion products after drying of NaCl droplet on carbon steel surface.

It can be concluded that the concentration of dissolved salts progressively increased towards saturation and the precipitation of the corrosion products being governed by the relative solubility and local concentration variations. The results obtained in our study are in good agreement with the model suggested by Venkatraman et al. [25] for rapid oxygen diffusion through fine droplets, and preventing oxygen depletion at the droplet center and driving the cathode reaction to the edge of the Fig. shows the photomicrograph of carbon steel after complete drying. The drop color turned brown due to the dissolution of the iron ions. The main phases constituting the corrosion products are: magnetite (Fe_3O_4), goethite ($\alpha\text{-FeOOH}$) and lepidocrocite ($\gamma\text{-FeOOH}$) as reported previously in the literature [26-39]. The phases are localized in a particular way in the rust layer: goethite was found in the inner layer and lepidocrocite more in the outer layer of the rust.

4. CONCLUSIONS

1- The new experimental set up described in this work has proven to be a suitable for monitoring the corrosion rate simultaneously with droplet height, contact angle and the volume loss under a single droplet of electrolyte.

2- The droplet height and contact angle continually dropped as droplet holding time progressed while the volume loss increased.

3- The droplet diameter remained practically constant over a holding lifetime of the drop.

4-The mechanism of corrosion process inside the droplet occurs through dissolution precipitation mechanism.

ACKNOWLEDGEMENT

The project was supported by King Saud University, Deanship of Scientific Research, Research Chair.

References

1. T. Tsuru, K.I. Tamiya, A. Nishikata, *Electrochim. Acta* 49 (2004) 2709.
2. J. Wang, J. Zhang, The Effect of Micro-droplets Formation Caused by the Deliquescence of the Deposited Salt Particle on Atmospheric Corrosion of Metals; Proc. 16ICC, No. 5-B-10, Beijing, CHINA, September 19–24, 2005.
3. J. Zhang, J. Wang, Y. Wang, *Electrochem. Commun.* 7, 443 (2005) .
4. I.S. Cole, T.H. Muster, N.S. Azmat, M.S. Venkatraman, A. Cook, *Electrochim. Acta* 56, 1856 (2011).
5. W.C. Keene, R. Sander, A.P. Pszenny, R. Vogt, P.J. Crutzen, J.N. Galloway, *J. Aerosol. Sci.* 29, 339–356 (1998) .
6. S.L. Clegg, P. Brimblecombe, A.S. Wexler, *J. Phys. Chem. A* 102, (1998) 2137 .
7. I.S. Cole, N.S. Azmat, A. Kanta, M. Venkatraman, *Int. Mater. Rev.* 54 (2009). 117
8. C. Leygraf, T.E. Graedel, Atmospheric Corrosion, John Wiley & Sons, New York, 2000.
9. A. Topcu, S. Incecik, A.T. Atimtay, *Atmos. Res.* 65, (2002) 77–92.
10. U.R. Evans, Corrosion and Oxidation of Metals, Arnolds, London, 1960.
11. G A. EL-Mahdy¹, Amro K.F. Dyab¹, Hamad A. Al-Lohedan¹ *Int. J. Electrochem. Sci.*, 8, (2013) 5232 .
12. G.A. El-Mahdy, A. Nishikata, T. Tsuru, *Corros. Sci.* 42, (2000) 183 .
13. G.A.EL-Mahdy, A.Nishikata and T.Tsuru *Corros. Sci.* 42, (2000) 1509.
14. G. A. EL – Mahdy and Kwang B. Kim *Corrosion* 63 (2007) 171 .
15. G. A. EL-Mahdy and Kwang B. Kim *Electrochemistry* 75, (2007) 403.
16. G. A. EL – Mahdy *Corros. Sci.* 47 (2005) 1370.
17. G. A. EL – Mahdy (2005) *J. App. Electrochem.* 35 (2005) 347.
18. G. A. EL – Mahdy and Kwang B. Kim *Corrosion* 61 (2005) 420.
19. G. A. EL – Mahdy and Kwang B. Kim *Electrochim. Acta* 49 (2004) 1937.
20. G.A. El-Mahdy, *Corrosion* 59 (2003) 505.
21. G A. EL-Mahdy¹, Amro K.F. Dyab¹, Ayman M. Atta, Hamad A. Al-Lohedan¹ *Int. J. Electrochem. Sci.*, 8 (2013) 9858.
22. G A. EL-Mahdy¹, Amro K.F. Dyab¹, Ayman M. Atta, Hamad A. Al-Lohedan¹ *Int. J. Electrochem. Sci.*, 8 (2013) 9992 .
23. M. Stern, A.L. Geary, *J. Electrochem. Soc.* 104 (1957) 56 .
24. N.S. Azmat, K.D. Ralston, B.C. Muddle, I.S. Cole, *Corros. Sci.* 53 (2011) 1604.
25. M.S. Venkatraman, I.S. Cole, D.R. Gunasegaram, B. Emmauel, *Mater. Sci. Forum* 654–656 (2010) 1650.
26. K. Kashima, S. Hara, H. Kishikawa, H. Miyuki, *Corros. Eng.* 49 (2000) 25.
27. M. Yamashita, H. Miyuki, Y. Matsuda, H. Nagano, T. Misawa, *Corros. Sci.* 36 (1994) 283.
28. M. Yamashita, H. Miyuki, H. Nagano, *Sumitomo Search* 57 (1995) 12.
29. H. Katayama, M. Yamamoto, T. Kodama, *Corros. Eng.* 49 (2000) 77.
30. M. Takemura, S. Fujita, K. Morita, K. Sato, *J.-I. Sakai*, 49 (2000) 111 .
31. P. Keller, *Werkst. Korros.* 18 (1967) 865.
32. T. Misawa, K. Hashimoto, S. Shimodaira, *Corros. Sci.* 14, 279 (1974) 14.

33. A. Raman, B. Kuban, A. Razvan, *Corros. Sci.* 32 (1991) 1295.
34. H. Fujiwara, T. Sugano, M. Aosawa, T. Nagatani, *Corros. Eng.* 49 (2000) 145.
35. M. Yamashita, T. Misawa, *Corros. Eng.* 49 (2000) 159.
36. J.W. Stewart, J.A. Charles, E.R. Wallach, *Mater. Sci. Technol.* 16 (2000) 283 .
37. D. Neff, P. Dillmann, *Nucl. Instrum. Methods Phys. Res. B* 181 (2001) 675.
38. R. Balasubramaniam, A.V. Ramesh Kumar, *Corros. Sci.* 42 (2000) 2085.
39. Ph. Dillmann , F. Mazaudier , S. Hoerle *Corros. Sci.* 42 (2004) 1401.

© 2014 The Authors. Published by ESG (www.electrochemsci.org). This article is an open access article distributed under the terms and conditions of the Creative Commons Attribution license (<http://creativecommons.org/licenses/by/4.0/>).